Soft Materials

ISSN: 1539-445X (Print) 1539-4468 (Online) Journal homepage: http://www.tandfonline.com/loi/lsfm20

Temperature-sensitive biocompatible IPN hydrogels based on poly(NIPA-PEGdma) and photocrosslinkable gelatin methacrylate

Ana Agustina Aldana, María Isabel Rial-Hermida, Gustavo Abel Abraham, Angel Concheiro & Carmen Alvarez-Lorenzo

To cite this article: Ana Agustina Aldana, María Isabel Rial-Hermida, Gustavo Abel Abraham, Angel Concheiro & Carmen Alvarez-Lorenzo (2017) Temperature-sensitive biocompatible IPN hydrogels based on poly(NIPA-PEGdma) and photocrosslinkable gelatin methacrylate, Soft Materials, 15:4, 341-349, DOI: 10.1080/1539445X.2017.1378677

To link to this article: http://dx.doi.org/10.1080/1539445X.2017.1378677

Accepted author version posted online: 18 Sep 2017.
Published online: 18 Sep 2017.

SOFT MATERIALS
2017, VOL. 15, NO. 4, 341–349
https://doi.org/10.1080/1539445X.2017.1378677

Taylor & Francis
Taylor & Francis Group

Temperature-sensitive biocompatible IPN hydrogels based on poly (NIPA-PEGdma) and photocrosslinkable gelatin methacrylate

Ana Agustina Aldana [a], María Isabel Rial-Hermida[b], Gustavo Abel Abraham [a], Angel Concheiro [b], and Carmen Alvarez-Lorenzo [b]

[a]Instituto de Investigaciones en Ciencia y Tecnología de Materiales, INTEMA (UNMdP-CONICET), Mar del Plata, Buenos Aires, Argentina; [b]Departamento de Farmacología, Farmacia y Tecnología Farmacéutica, R+DPharma Group (GI-1645), Facultad de Farmacia, Universidade de Santiago de Compostela, Santiago de Compostela, Spain

ABSTRACT

The future of tissue engineering and regenerative medicine relies on the development of biomimetic extracellular matrices (ECM). Hydrogels based on biological and synthetic macromolecules could mimic native ECM which is an interpenetrating network (IPN) of proteins and other biomacromolecules. In this study, gelatin and N-isopropylacrylamide-based IPN hydrogels, named as NPxG, were developed to fabricate 3D matrix systems. A series of IPN hydrogels with different contents in poly(NIPA-PEGdma) (NPx) and gelatin methacrylate (GelMA) were synthesized. NPx and GelMA were characterized by Habeeb's assay, FTIR, and ^{1}H-NMR. IPN hydrogels were fully characterized by ATR-FTIR, swelling measurements, optical microscopy, SEM, DSC, and rheology. Optical microscopy images and rheology demonstrated that hydrogel properties change around 37°C. Above LCST, the translucent colorless hydrogel shifted to an opaque white hydrogel and the storage modulus increased. A wide range of IPN gels with different swelling properties and potential applications in different fields can be produced by controlling experimental parameters.

ARTICLE HISTORY
Received 22 August 2017
Accepted 8 September 2017

KEYWORDS
Interpenetrating network; gelatin; thermosensitive hydrogels; cell culture

Introduction

Recent achievements and future advancements in tissue engineering and regenerative medicine rely on the engineering of biomimetic extracellular matrices (ECM). Native ECM has a heterogeneous and hierarchical network architecture that surrounds cells, providing mechanical support and a biologically interactive environment that facilitates both cellular and organ function. Native ECM is an interpenetrating network (IPN) of crosslinked proteins interlaced with high-molecular-weight biomacromolecules. Popular approaches for replicating ECM composition utilize physically or chemically crosslinked hydrogels composed of a wide range of biological and synthetic macromolecules (1, 2).

Several kinds of materials have been developed for hydrogel scaffolds. Hydrogels based on synthetic polymers, such as poly(ethylene glycol) (PEG), poly(vinyl alcohol) and poly(acrylic acid), are compositionally consistent, nontoxic, hydrophilic and possess controllable chemical and mechanical properties. However, these synthetic materials lack biologically active sites and extensive conjugation chemistry is required to introduce bioactive molecules such as RGD peptides (arginine–glycine–aspartic acid) to promote cell response. Scaffolds derived from natural biomacromolecules such as collagen, gelatin, chitosan, and hyaluronic acid can actively support cell proliferation, migration, and differentiation. However, these materials are hard to process, exhibit weak mechanical properties, and the obtained products are poorly reproducible. To overcome these limitations, the combination of naturally derived and synthetic materials represents an attractive approach to create scaffolds for tridimensional cell culture (3).

Gelatin is an inexpensive material obtained from denatured collagen, and presents integrin cell-binding motifs, such as RGD, and matrix metalloproteinases (MMP) degradable sites. Compared to native collagen, gelatin has lower antigenicity and less batch-to-batch variation due to the denaturation process, in which tertiary protein structures are removed. Conjugation of methacrylate groups to the amine-containing groups of gelatin (GelMA) provides a photopolymerizable biomaterial that has been widely investigated for cell-based studies and tissue engineering applications. Crosslinking of the methacrylic side groups results in hydrogels with stiffness and density that can be

CONTACT Ana Agustina Aldana aaldana@fi.mdp.edu.ar Instituto de Investigaciones en Ciencia y Tecnología de Materiales, INTEMA (UNMdP-CONICET), Av. Juan B. Justo 4302, B7608FDQ, Mar del Plata, Buenos Aires, Argentina.

controlled by varying the polymer dry mass, degree of functionalization, photo-initiator concentration, ultraviolet (UV) intensity and exposure time. Photo-chemical crosslinking takes place only in the presence of a photo-initiator, and thus hydrogel formation is triggered by the external source of UV light. Irgacure 2959 is usually chosen as photoinitiator due to its low toxicity at the used concentration as demonstrated in previous studies (4–6).

On other hand, temperature-responsive synthetic polymers, such as poly(N-isopropylacrylamide) (pNIPA), have been demonstrated to be excellent tools for tuning interactions of cells with a substrate and also to form depots in a tissue for the sustained release of encapsulated drugs or gene vectors (7, 8). At low temperature, pNIPA chains are hydrophilic, but a sudden increase in hydrophobicity is observed at a temperature close to 31°C, known as low critical solubility temperature (LCST), which causes the polymer to precipitate. The temperature and the thermodynamics of the phase transition of poly(N-isopropylacrylamide)-based physical gels can be altered by incorporation of various comonomers. For example, mixtures of poly (polyethylene glycol citrate-co-N-isopropylacrylamide) with gelatin have intrinsic antioxidant properties and an LCST slightly lower than that of pNIPA and perform as suitable injectable depots for regenerative medicine; the presence of gelatin ensured cell viability and differentiation (9). Moreover, changes in temperature can be exploited for selective cell adhesion/detachment from scaffolds prepared with pNIPA grafted with gelatin (10, 11). In the case of IPN, the pNIPA network maintain its main properties nearly unaltered although the nature and structure of the other network may also play a role in the thermodynamics of the transition (12). In a previous work, IPNs prepared by first synthesizing the pNIPA network in the presence of gelatin, followed by cross-linking of the protein with glutaraldehyde, exhibited the volume phase transition at the same temperature as pNIPA hydrogels although the magnitude of the changes was less (13). Changes in swelling, porosity, surface hydrophobicity and mechanical properties associated to the temperature-triggered phase transition could be exploited to tune the performance of the IPN networks as scaffolds and as drug delivery systems (14). Nevertheless, there is still a paucity of information on the performance of full IPNs of pNIPA and cross-linked gelatin (15).

The aim of this study was to prepare gelatin and N-isopropylacrylamide-based interpenetrating networks (NPxG) that can be suitable as biocompatible matrices for tissue engineering. To prepare the NPxG, first cross-linked hydrogels of pNIPA and poly (ethylene glycol) dimethacrylate (PEGdma) were prepared. For the gelatin network, the use of glutaraldehyde was avoided and gelatin methacrylate was prepared and cross-linked under mild photopolymerization conditions, which have been demonstrated to render highly biocompatible scaffolds (16). Structural and physical properties of the NP*x*G IPNs as well as their ability to support cell growth were investigated.

Experimental

Materials

Gelatin type A (Sigma Aldrich); methacrylic anhydride (MA, Sigma Aldrich); *N*-isopropylacrylamide (NIPA, Sigma Aldrich); poly(ethylene glycol) dimethacrylate (PEGdma, Mn = 550, Aldrich); ammonium persulfate (APS, Sigma Aldrich); N,N,N',N'-tetramethylenediamine (TEMED, Sigma Aldrich). Irgacure 2959 (I2959) was obtained from BASF and used as photoinitiator. Human adipose-derived stem cells (MSC) StemPRO, MesenPRO RS^{TM} Basal Medium, and MesenPRO RS^{TM} Growth Supplement were acquired from Gibco, Invitrogen (CA, USA). L-Glutamine was purchased from Sigma Aldrich (Germany). LIVE/DEAD® viability/cytotoxicity Kit was obtained from Life Technologies (MA, USA). Penicillin/streptomycin was acquired from ThermoScientific HyClone, Fisher Scientific (UK). Cell Proliferation Kit I (MTT) was purchased from Roche (Switzerland).

Synthesis of methacrylated gelatin (GelMA)

GelMA was prepared by adding 8 mL of methacrylic anhydride to 10 g of gelatin in 100 mL of MilliQ water during 2 h with magnetic stirring at 50°C. The mixture was dialyzed by using a 12–14 kDa cutoff membrane in distilled water for one week at 40°C, and then freeze-dried for 72 h. The degree of methacrylation, defined as the percent of amine groups converted to methacrylamide groups, was determined by Habeeb's test (17). GelMA was characterized by ^{1}H-NMR and FTIR spectroscopy.

Synthesis of poly(nipa-pegdma) networks

Hydrogel networks were prepared by free radical polymerization in aqueous solution using *N*-isopropylacrylamide (NIPA) as a monomer, poly (ethylenglycol) dimethacrylate (PEGdma) as a cross-linking agent, and the redox couple APS/TEMED as an initiator. In a typical procedure, the monomer (5% w/v), crosslinking agent (4, 2, 1 or 0.5% of PEGdma

mole respect to NIPA mole) and 4% w/v APS solution (250 µL) were dissolved in 4.5 mL of MilliQ water in a tube and shaken with a vortex. Then, nitrogen was bubbled for 5 min to deoxygenate the system and finally, 250 µL TEMED was added. The reactions were carried out for 20 h at 25°C. After reaction, highly viscous gels were obtained. Each product was dialyzed against distilled water to remove residual unreacted monomers, and then freeze-dried. The products obtained were named NP*x*, where *x* is the molar relation of PEGdma respect to NIPA. The experimental conditions to yield the products are summarized in Table 1.

Preparation of IPN hydrogels

First, a solution of GelMA (10.0% w/v in MilliQ water) and photoinitiator (0.75% w/v I2959) was prepared in a tube and heated at 60°C for 1 h. The NP*x* swollen networks (10.0% w/v in MilliQ water) were prepared in separate. Both GelMA macromonomer and NP*x* networks were mixed (compositions in Table 2) and poured into the wells of a 48-well culture plate that were used as molds. The system was exposed 50 min to UV light (360 nm) for curing of GelMA. After that, the plate was taken to the fridge for 24 h. Finally, the hydrogels were unmolded carefully from each well and washed exhaustively with MilliQ water and phosphate buffer solution (PBS, pH 7.4) to remove residual photoinitiator. The hydrogel discs were freeze-dried for further studies. The products obtained were named NP*x*G where NP*x* is the NIPA-based gel network and Gel-C is a crosslinked GelMA network. NP4 and NP0.5 did not render homogeneous systems when mixed with GelMA and, therefore, NP4G and NP0.5G were discarded.

Table 1. Monomer composition of the prepared NPx gel networks.

NP*x* network	NIPA (g)	PEGdma (µl)
NP4	0.25	44
NP2	0.25	22
NP1	0.25	11
NP05	0.25	5.5

Table 2. Components used to prepare NP*x*G IPNs.

	PN*x*			
IPN	Code	(mL)	GelMA (mL)	I2959 (%w/v)
Gel-C	–	–	10	0.75
NP4G	NP4	3.3	6.7	0.5
NP2G	NP2	3.3	6.7	0.5
NP1G	NP1	3.3	6.7	0.5
NP05G	NP05	3.3	6.7	0.5

Discs of dried IPNs were re-hydrated in MilliQ water and maintained at different temperatures (4, 25, 35, and 40°C) during 2 h at each temperature. After this period, pictures were taken. The IPNs with 1:2 weight ratios changed their opacity with temperature and these IPNs were chosen for their following characterization.

FTIR and NMR analysis

Fourier Transform Infra-Red Spectroscopy (FTIR) was performed with the Nicolet 6700 spectrophotometer (Nicolet Instruments Inc., WI, USA) using attenuated total reflectance (ATR) mode. Spectra were obtained over a range of 600–4000 cm^{-1} at a resolution of 2 cm^{-1} at room temperature.

^{1}H NMR spectra of NP*x* networks (NP05, NP1, NP2, and NP4) swollen in D_2O were recorded using a Bruker DRX-500 (USA) nuclear magnetic resonance spectrometer operating at 500 MHz at 298 K.

Thermal properties

Differential scanning calorimetry (DSC) analyses were performed using a DSC Q100 (TA Instruments, New Castle, DE, USA) calorimeter. DSC runs were conducted in a hermetic sealed aluminum pans at a heating rate of 10°C/min in the range of 0–300°C, under nitrogen atmosphere.

Morphological characterization

The structural morphology of the IPNs was examined by scanning electron microscopy (SEM, Zeiss FESEM Ultra Plus, Germany). The lyophilized IPNs were coated with gold using a sputter coater and imaged with SEM at 20 kV.

Swelling

The swelling behavior of the IPNs was studied by immersing each dried disc (12 mm diameter and 3 mm thickness) in 1 ml PBS at different temperatures and kept under oscillatory movement (orbital shaker, 60 rpm). At predetermined time points, the IPNs were retrieved and then weighed after their surfaces were blotted with filter paper. Then, they were returned to the corresponding vials. The process was repeated every hour until a constant swelling weight was obtained and the swelling (S) was quantified as follows:

$$S(\%) = [(W - W_0)/W_0] \cdot 100 \quad (1)$$

where W_0 and W represent the initial weight of the dried disc and the weight after swelling, respectively.

Rheology

Viscoelastic properties of NP2G, NP1G, and Gel-C hydrogel discs were recorded under oscillatory shear deformation in an Anthon Paar rheometer using parallel rough plates of 25 mm diameter (gap close to 2 mm). Mechanical spectra were recorded in a constant strain mode, with a deformation of 0.5% and constant normal force of 1 N maintained over the frequency range of 0.1 to 100 Hz at 20°C. The temperature dependence of the storage (elastic) modulus (G') was determined applying a temperature scan ranging from 20 to 50°C (heating rate 1°C/min) at constant frequency (1 Hz), amplitude (0.5%), and shear stress (0.05 N).

Cell proliferation

Pieces of scaffolds of 0.4 x 0.4 cm^2 were incubated with MesenPro supplemented with 1% penicillin/streptomycin, 1% L-glutamine, and 2% growth supplement during 24 h for swollen of the IPNs. The day before the assay, MSC were seeded at rate of 10000 cells per well into 0.5 mL of medium in 48 wells plate. Scaffolds were placed in contact with cells and 0.5 mL of culture medium was added. After 1, 3 and 7 days, proliferation was quantified using a MTT kit according to the manufacture instructions.

Results and discussion

Synthesis of gelatin methacrylate (GelMA) and poly (nipa-pegdma)

GelMA was synthesized according to previously reported methods, in which methacrylate functional groups were grafted onto the gelatin backbone through reaction between methacrylic anhydride and lysine residues (Fig. 1) (5, 6). The GelMA infrared spectrum (Fig. 1b) showed peaks at 1645, 1526, and 1240 cm^{-1} related to the C = O stretching (amide I), N–H bending (amide II), and C–N stretching plus N–H bending (amide III), respectively. Moreover, a N–H stretching (amide A) could be observed at 3284 cm^{-1}. The MA modification was not detected by FTIR because the peaks of MA overlapped with gelatin peaks. ^{1}H-NMR spectrum of GelMA is shown in Fig. 1(c). The modification of lysine residues with methacrylate groups was confirmed by the decrease in the lysine signal at 2.9 ppm (y), and the appearance of the methacrylate group signal at 5.4 ppm and 5.7 ppm (x) and the methyl group signal at 1.8 ppm (z) (18). A degree of methacrylation of 71% was calculated using Habeeb's test (17).

On the other hand, NP*x* gel networks were prepared by redox polymerization of NIPA with poly(ethylene glycol) dimethacrylate (PEGdma) (crosslinker) in water at room temperature (Fig. 2a). NP*x* networks were prepared with 5% w/v NIPA solution and different mole ratio of PEGdma respect to NIPA (0.5, 1, 2 and 4) (Table 2). Higher concentrations of NIPA were also explored, but the resultant systems were too viscous for mixing with GelMA in the following step.

^{1}H-NMR spectra of poly(NIPA-PEGdma) (NP*x*) is shown in Fig. 2(b). The spectra of pNIPA displayed peaks at 1.10, 1.53, 1.96, and 3.85 ppm corresponding to, respectively, $-CH_3$, $-CH_2-$, –CH–, and –CH(NH)– hydrogens of polymeric backbone. Same peaks and a new signal at 3.64 ppm corresponding to polyethylene glycol unit were observed for NP*x*. Moreover, ^{1}H-NMR

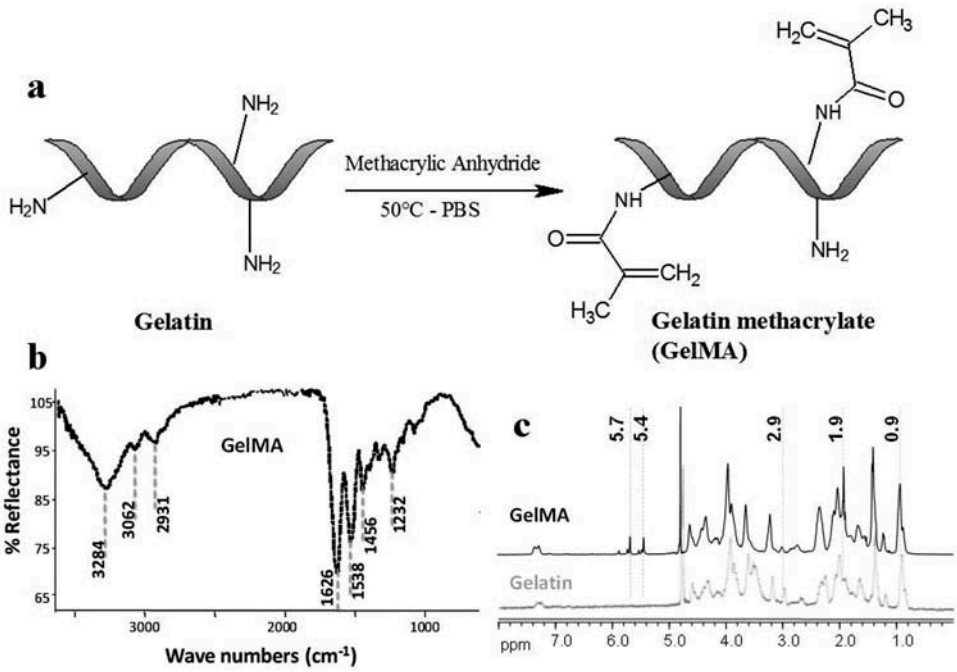

Figure 1. (a) Scheme of GelMA synthesis, (b) FTIR, and (c) ^{1}H-NMR spectra of GelMA.

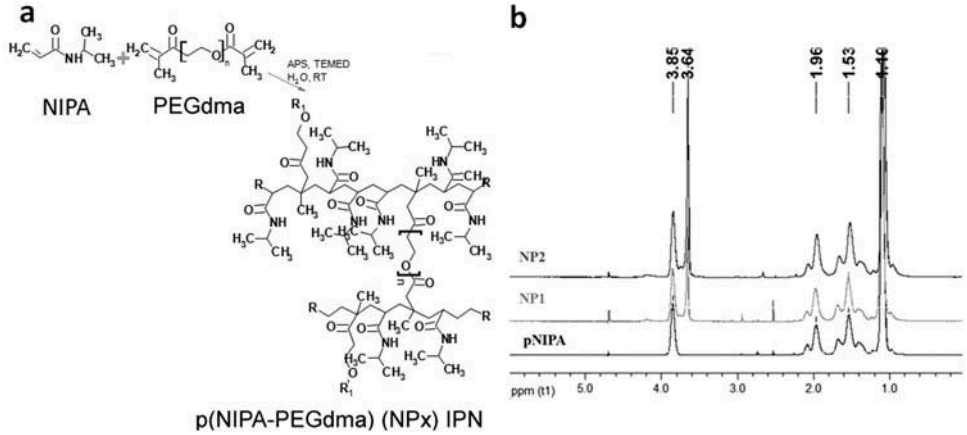

Figure 2. (a) Structure and (b) ^{1}H-NMR spectra of pNIPA and NP*x* networks.

spectra did not show vinyl group signal around 5 ppm indicating a complete polymerization reaction. As expected, the intensity of peaks attributed to PEG increased as the amount of PEG increased.

Synthesis and characterization of IPN hydrogels

Once NP*x* and GelMA were obtained, the method to prepare NP*x*G IPNs was optimized. GelMA-photoinitiator and NP*x* gel networks were mixed before crosslinking under UV irradiation. The 10% w/v final polymer solution with different mass ratio between GelMA and NP*x* were prepared and the irradiation time was 50 min at 360 nm (Fig. 3a). NP1 and NP2 gels allowed obtaining IPNs because their good miscibility with GelMA solution. NP05G led to too weak IPNs, while NP4G caused the IPNs to separate into two layers. Therefore, NP05G and NP4G were discarded for subsequent studies.

ATR-FTIR spectra of poly(NIPA-PEGdma), NP2G and Gel-C (crosslinked GelMA hydrogel) samples are shown in Fig. 3(b). The NP*x*G spectrum presented peaks typical of poly(NIPA) and Gel-C, showing that the resulting IPN hydrogel contained both components. The band at 2971 cm^{-1} indicated the presence of poly (NIPA) in IPN hydrogel. Moreover, the NP*x*G showed peaks at 1125 and 1072 cm^{-1} related to the C–O–C group vibration. The other prepared IPN hydrogels showed a similar ATR-FTIR spectrum.

The cross-sectional microstructures of freeze-dried hydrogels were examined by SEM (Fig. 3c). SEM micrographs of the NP*x*G IPNs showed distinctive changes in microstructure that depended on the degree of crosslinking of NP*x*. Gel-C hydrogel exhibited petal-shaped porous

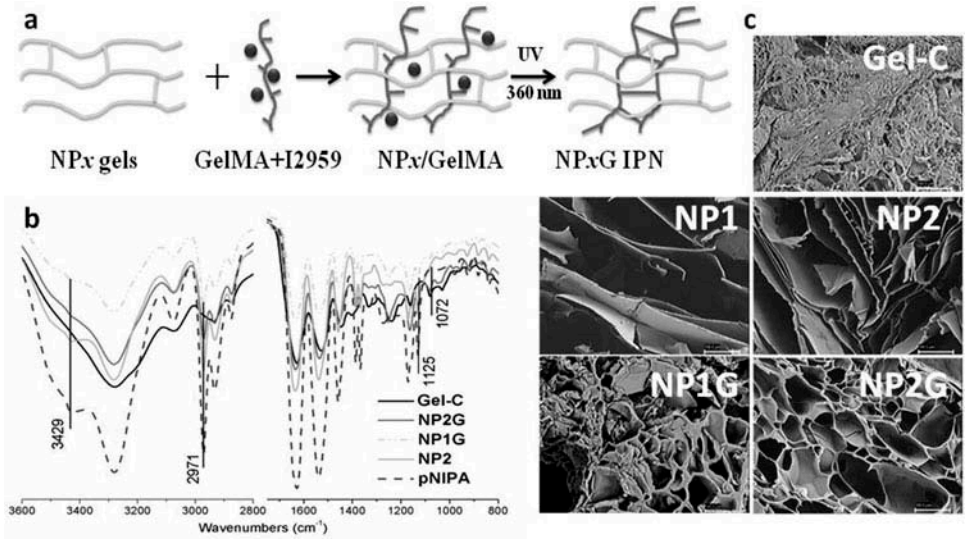

Figure 3. (a) Scheme of the NP*x*G IPNs preparation. (b) ATR-FTIR spectra of pNIPA, NP2G, NP1G, NP2, and Gel-C. (c) SEM micrographs of NP1, NP2, NP1G, NP2G, and Gel-C (scale bar 100 μm).

morphology; whereas, the NP*x*G and NP*x* hydrogels showed clearly defined network structures. NP2 and NP1 hydrogels presented several parallel sheets. These parallel sheets were filled with GelMA in the IPN hydrogel (Fig. 3c). For the NP2G and NP1G IPNs, the wall thickness of material surrounding the pores was greater than in NP2 and NP1 hydrogels, respectively, and the porous structure changed. The hydrogel structure looked like Gel-C hydrogel when GelMA percentage increased in the IPN.

Optical micrographs of NP*x*G incubated at 4, 25, 37, and 40°C for 2 h evidenced that the IPNs exhibit temperature-responsive behavior (Fig. 4). NP2G and NP1G IPNs were transparent at 37°C or below, but became opaque when the water temperature raised to 40°C. Differently, the Gel-C hydrogel remained transparent at all temperatures.

The swelling was also recorded at various temperatures (Fig. 5). Gel-C swelling did not change with temperature. In contrast, NP*x*G IPNs underwent shrinking as the temperature increased above 30°C. Temperature-responsiveness was more marked for NP2G than for NP1G, which may be related to the attenuation of the volume phase transition due to the interpenetration by Gel-MA. Probably, the gelatin chains interpenetrated better into NP1 than NP2 and thus led to microdomains in which pNIPA chains are partially isolated and the cooperative intermolecular bonding is attenuated (12).

DSC scans of Gel-C, NP2, and N2P5G are shown in Fig. 6. The Gel-C thermogram showed endothermic peaks at 116 and 221°C, which are related to the denaturation and further thermal decomposition of gelatin. NP2 polymers presented a glass transition at 83°C with an endpoint at 121°C. The IPN exhibited peaks similar to both Gel-C and NP2. The endothermic peak of Gel-C was shifted at 165°C and decreased for both NP2G and NP1G. In addition, the intensity of peak at 165°C was significantly reduced for NP1G indicating a less degradation at this temperature, which may be related to better interpenetration of gelatin into NP1 than into NP2. The glass transition of NIPA was observed in both NP1G and NP2G IPNs.

The rheological properties of IPNs were analyzed monitoring the storage modulus as a function of temperature (Fig. 7). The storage modulus value of the Gel-C hydrogel remained constant independent of temperature. Differently, the rheological properties of NP1G and NP2G depended on temperature. At temperature below LCST of NIPA, water could act as lubricant or plasticizer between NIPA chains improving their mobility and thus reducing G'. As the temperature increases, the hydrophobic

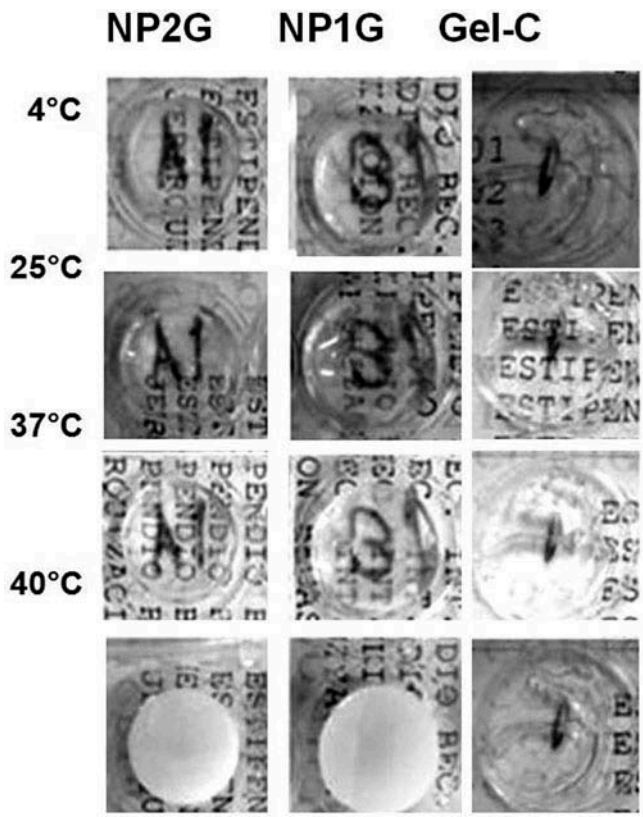

Figure 4. Optical micrographs of hydrogels at different temperatures: NP2G, NP1G, and Gel-C.

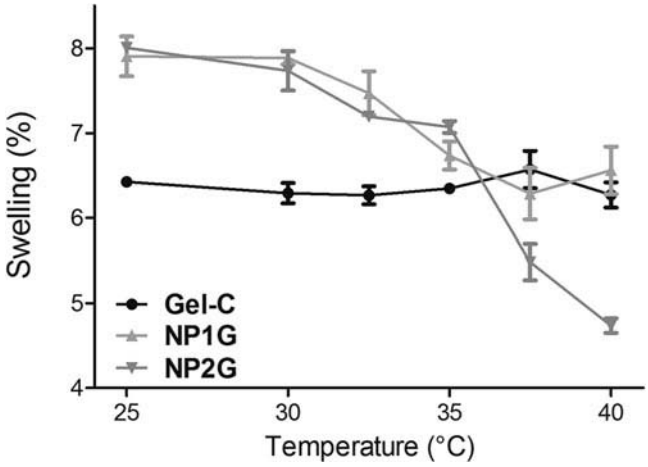

Figure 5. Swelling as a function of temperature of the Gel-C hydrogel, NP1G, and NP2G IPNs.

interaction becomes more important and water is displaced increasing the stress needed to mobilize the NIPA chains and thus G' increases. The magnitude of the increase of G' was larger for NP1G than for NP2G, probably due to low crosslinking and thus better mobility between NIPA chains. When temperature increases, NP1G shows higher G' than NP2G. The transition temperature of the storage modulus was around 34°C for both NP1G and NP2G.

Cell proliferation

Mesenchymal stem cell (MSC) viability and proliferation were evaluated seeding cells on Gel-C, NP1G, and NP2G hydrogels. Several studies have shown that gelatin hydrogels with porous structure are cytocompatible with several cells lines (19). In our study, the greatest proliferation of MSC was recorded at day 3 (Fig. 8). No relevant differences were observed between gelatin hydrogel and the IPNs confirming that the NP network did not cause detrimental effects on cytocompatibility. The decrease in proliferation recorded at 7th day could be due to the limited space for proliferation.

Conclusions

Gelatin and N-isopropylacrylamide-based interpenetrating networks can be easily prepared in aqueous medium by means of photopolymerization. IPNs showed macropores of the pNIPA network partially occupied by the gelatin network rendering a variety of pore sizes that could be advantageous for cell adhesion and proliferation. IPNs were temperature-responsive, but the responsiveness became attenuated for those with lower content in pNIPA (due to an increase in PEGdma). A wide range of IPN gels with different swelling properties and potential applications in different fields can be produced through the correct control of the different experimental parameters.

Acknowledgments

A.A. Aldana thanks CONICET for a postdoctoral scholarship.

Funding

This work was supported by the Argentinean National Agency of Scientific and Technological Promotion (PICT 224), and CONICET (PIP 0089). CYTED (RIMADEL network of the Ibero-American Program for Science, Technology and Development) and Xunta de Galicia (Axudas para Grupos de Referencia Competitiva ED431C 2016-PG020) are also acknowledged.

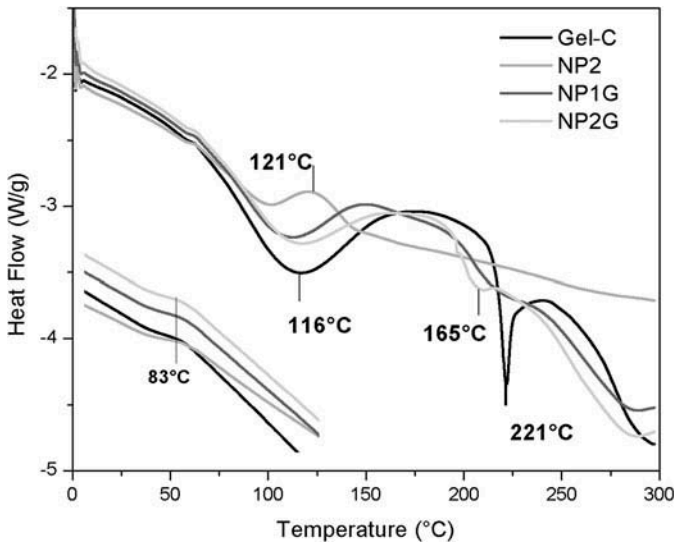

Figure 6. DSC scans of Gel-C, NP2, NP2G, and NP1G.

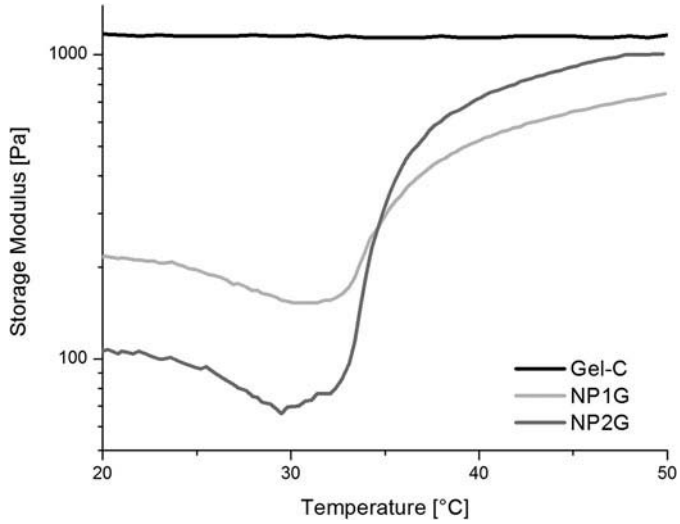

Figure 7. Storage modulus as a function of temperature for Gel-C, NP2G, and NP1G.

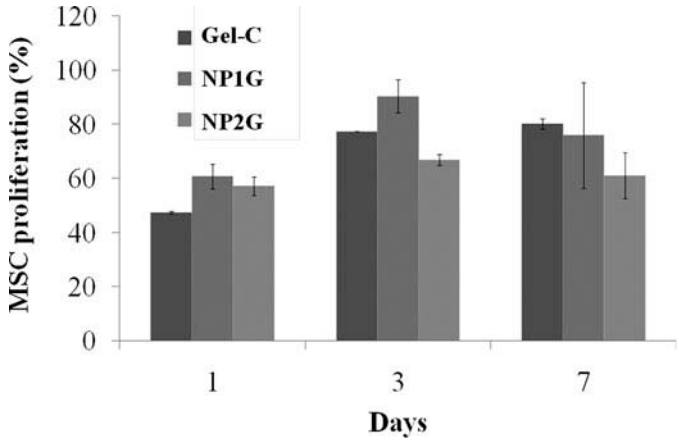

Figure 8. MSC proliferation on Gel-C, NP1G, and NP2G hydrogels.

ORCID

Ana Agustina Aldana http://orcid.org/0000-0003-4997-7982
Gustavo Abel Abraham http://orcid.org/0000-0001-7094-1031
Angel Concheiro http://orcid.org/0000-0003-0507-049X
Carmen Alvarez-Lorenzo http://orcid.org/0000-0002-8546-7085

References

1. Daniele, M.A., Adams, A.A., Naciri, J., North, S.H., and Ligler, F.S. (2014) *Biomaterials*, 35:1845–1856.
2. Mellati, A., Fan, C.M., Tamayol, A., Annabi, N., Dai, S., Bi, J.X., Jin, B., Xian, C., Khademhosseini, A., and Zhang, H. (2017) *Biotechn Bioengineering*, 114:217–231.
3. Xu, K., Fu, Y., Chung, X., Zheng, X., Cui, Y., Hsu, I.C., and Kao, W.J. (2012) *Acta Biomaterials*, 8:2504–2516.
4. Van Den Bulcke, A.I., Bogdanov, B., Cornelissen, M., Schacht, E.H., De Rooze, N., and Berghmans, H. (2000) *Biomacromolecules*, 1:31–38.
5. Hutson, C.B., Nichol, J.W., Aubin, H., Bae, H., Yamanlar, S., Al-Haque, S., Koshy, S.T., and Khademhosseini, A. (2011) *Tiss Engineering A*, 17:1713–1723.
6. Nichol, J.W., Koshy, S.T., Bae, H., Hwang, C.M., Yamanlar, S., and Khademhosseini, A. (2010) *Biomaterials*, 31:5536–5544.
7. Alexander, A., Ajazuddin, K.J., Saraf, S., and Saraf, S. (2014) *European Journal Pharma Biopharmaceuticals*, 88:575–585.
8. Chen, L.N., Xie, Z., Gan, T.S., Wang, Y., Zhang, G.Z., Mirkin, C.A., and Zheng, Z.J. (2016) *Small*, 12:3400–3406.
9. Dumanian, Z.P., Tollemar, V., Ye, J., Lu, M., Zhu, Y., Liao, J., Ameer, G.A., T-Ch., H., and Reid, R.R. (2017) *PLoS One*, 12:e0172327.
10. Zhao, X.M., Wang, L., Wang, P.L., Yang, Y., and Wang, F. (2016) *Journal of Nanoscience and Nanotechnology*, 16:5520–5527.

11. Ren, Z.W., Wang, Y., Ma, S.Q., Duan, S., Yang, X.P., Gao, P., Zhang, X., and Cai, Q. (2015) *ACS Applied Material Interfaces*, 7:19006–19015.
12. Alvarez-Lorenzo, C., Concheiro, A., Dubovik, A.S., Grinberg, N.V., Burova, T.V., and Grinberg, V.Y. (2005) *Journal Control Release*, 102:629–641.
13. Dhara, D., Rathna, G.V.N., and Chatterji, P.R. (2000) *Langmuir*, 16:2424–2429.
14. Lima, A.C., Song, W., Blanco-Fernandez, B., Alvarez-Lorenzo, C., and Mano, J.F. (2011) *Pharmaceutical Research*, 28:1294–1305.
15. Rathna, G.V.N., and Chatterji, P.R. (2001) *Journal Macromol Sciences*, 38:43–56.
16. Eke, G., Mangir, N., Hasirci, N., and Hasirci, M.S. (2017) *Biomaterials*, 129:188–198.
17. Habeeb, A.F.S.A. (1966) *Analytical Biochemistry*, 14:328.
18. Nguyen, A.H., McKinney, J., Miller, T., Bongiorno, T., and McDevitt, T.C. (2015) *Acta Biomaterials*, 13:101–110.
19. Dubruel, P., Unger, R., Van Vlierberghe, S., Cnudde, V., Jacobs, P.J.S., Schacht, E., and Kirkpatrick, C.J. (2007) *Biomacromolecules*, 8:338–344.